International Journal of Research in Geography (IJRG)
Volume 1, Issue 1, June 2015, PP 29-37
www.arcjournals.org

Spatial Approach for Modeling Tropospheric Ozone and Its Interaction with the Infrared Wave and Temperature in Bogotá, Colombia

CASTRO-DIAZ, Ricardo

Research Program in Environment and Natural Resources – Institute of Geography
"Dr. Romualdo Ardissone"– University of Buenos Aires
Buenos Aires, Argentina
ircastrod@unal.edu.co

Abstract: *The human activities increase the global emissions, especially those resulting from industrial activities in urban areas. The tropospheric ozone, which is a pollutant derived from the interaction of the chemical smog under the solar radiation impact, is being analyzed because of its palliative effect to the greenhouse phenomenon.The situation becomes strongly dangerous due to the consequences to the public sanitation and the radiative forcing increasing the superficial temperature under the cities' smog. This layer retains the infrared and thermal waves causing a heat island effect.This research led a mixed methodology to combine the ETM+ sensor and the climate ground stations for describing the interaction between the urban pollution layer and the heat island phenomenon. A per-day 'local' dimming model was developed under four assumptions in order to understand the dynamics of the tropospheric ozone and the high temperatures.*

Keywords: *Tropospheric ozone, heat island effect, local dimming, ETM+ sensor, climate change.*

1. INTRODUCTION

During the last decade the nations around the world have ratified agreements for stimulating and promoting the reduction of the pollution emissions: Framework Convention on Climate Change (1992), Montreal Protocol (1987) and Kyoto Protocol (2005), which was postponed until 2020 for the Bali Action Plan in 2007.This last one includes the selective and joint decreasing specification for six gases causing the greenhouse effect: carbon dioxide (CO_2), methane gas (CH_4), nitrous oxide (N_2O), hydrofluorocarbons (HFCs), perfluorocarbons (PFCs) and sulfur hexafluoride (SF_6) in 5% between 2008 and 2012 compared with 1990.

These pollutants are the main causing agents of the global warming [1].They produce an atmospheric cover that retains the outgoing radiation between atmosphere and earth surface increasing the superficial temperature [2].

Even though the nations are taking actions, the uncertainty increases with the political and economic crisis periods like the 2000's represented to the world [3]. In the other hand, with the expecting reduction of the aerosols in the atmosphere driven by the Kyoto Protocol, other gases derived from multiple human activities, like water vapor and troposphere ozone, are highly contributing to the radiative forcing of the climate change.

In the period 1979-2005, the water vapor increase cannot be explained without the human activity impacts causing the amplification of the warming effect in the world climate system [4].Schmidt et al. [5] presented a combination of trends in El Niño, the representation of the aerosols, the volcanic and solar impacts explaining the errors and discrepancies in the warming trend since 1992. This 'historical' discussion in the scientific panorama implies that the greenhouse gases cause an emergent window for understanding the extreme consequences of the pollutants beyond the Intergovernmental Panel on Climate Change framework [6]

Related to this, the importance for understanding the contamination dynamics, this article generates an approach to cycle of tropospheric ozone (O_3), which is produced by the interaction of nitrogen oxides, carbon monoxides and volatile organic compounds in the presence of sunlight. The industrial and

transport emissions as NO_2 and hydrocarbons in the Earth's surface are precursors of this pollutant [7].

Jaramilloet al. [8] found high correlations between the smog components as Nitrogen Oxides and VOC and the amount of the troposphere O_3 in solar radiation presence building a prediction model through the univariate time series analysis.

In this sense, the solar radiation in tropical areas (from 23.4378° N and 23.4378° S) like Central America, North of South America, Middle Africa and South East of Asia is mostly a 12 h period, only naturally interfered by clouds coming from seasonal variations and other external phenomena. This situation is relevant to the formation of the O_3, which is completely involved with the increasing of several respiratory diseases [9] [10] and impacts the plants photosynthesis of the most populated cities [11]

Stan hill and Cohen [12] agglutinated the term 'global dimming' for describing this phenomenon, which is caused by the incomplete combustion of several fossil fuels creating brighter clouds and reflecting the solar radiation back to space. However, this topic includes also the urban dimming, which differs from global dimming because even they have the same genesis (pollutants) and a radiative forcing, they are described in different atmosphere layers and ground scale. This means that the global dimming is related to higher atmosphere studies and the urban dimming is focused on the lower atmosphere research [13][14].

The dimming effect also known as global dimming was noticeable between 1964 and 1989, and it's related to the sites' population density indicating less solar radiation in urban areas in comparison to those rural [15]. Even though the industrial and urban activities create the smog-dimming layer increasing the temperature in cities [16], Tanaka et al. [17] warn that these phenomenons are not limited to the cities. Then, the atmospheric circulation is also intervening the pollutants transportation cycle in the global context as shown in [18].

The local dimming induces to a greenhouse effect at small scale, and it is produced by the smog layer covering large cities driven by the industrial and transportation activities. Its dynamic includes the absorption of the sun thermal radiation and its later emission by the urban surface; this sequence is truncated by the pollutants in the lower atmosphere causing the radiative forcing and the reduction of the incoming sunlight.

In order to obtain a spatial approach for modeling the interaction of the troposphere O_3 with the thermal infrared wave and the urban temperature patterns, a study field was carried out taking into account several large cities in the intertropical zone. This included the selection of high-lands cities as a parameter for enhancing the effect of exposure to ultra-violet rays and sunlight.

Also a time period was chosen for avoiding the effects of El Niño Southern Oscillation, derived from the Oceanic Niño Index –ONI- of the National Weather Service (National Oceanic and Atmospheric Administration of the United States of America) for reducing the rainy and cloud effects on the solar radiation. In this context, the city of Bogota in Colombia met the requirements by its location at 2.640 m.a.s.l. and the 2007 period as a moderate ENSO index from recent years.

The Bogota metropolitan area (4.6097 N, 74.0817 W centroid) has nearly 12 million inhabitants located in a high plateau embedded in the east Andes with a subtropical bimodal climate and the average temperature is 14.5 °C.

2. DATA

2.1 Ground Measurements

The ground measurements data were suitable in the month period of February to August (2007) from eleven weather stations managed by the Bogota Bureau Quality Air Net and Environment and the Hydrologic and Meteorological Institute. Six pollutants were analyzed for building a daily experimental model: 2.5 μ particulate matter (MP2.5), 10 μ particulate matter (MP10), sulfur monoxide (SO), total suspended particle (TSP), carbon monoxide (CO), sulfur dioxide (SO_2), nitrogen mono-oxides (NOx), troposphere ozone (O_3), global radiation, atmospheric pressure and direction and speed wind. The Figure1 shows the weather and air quality stations locations in the city.

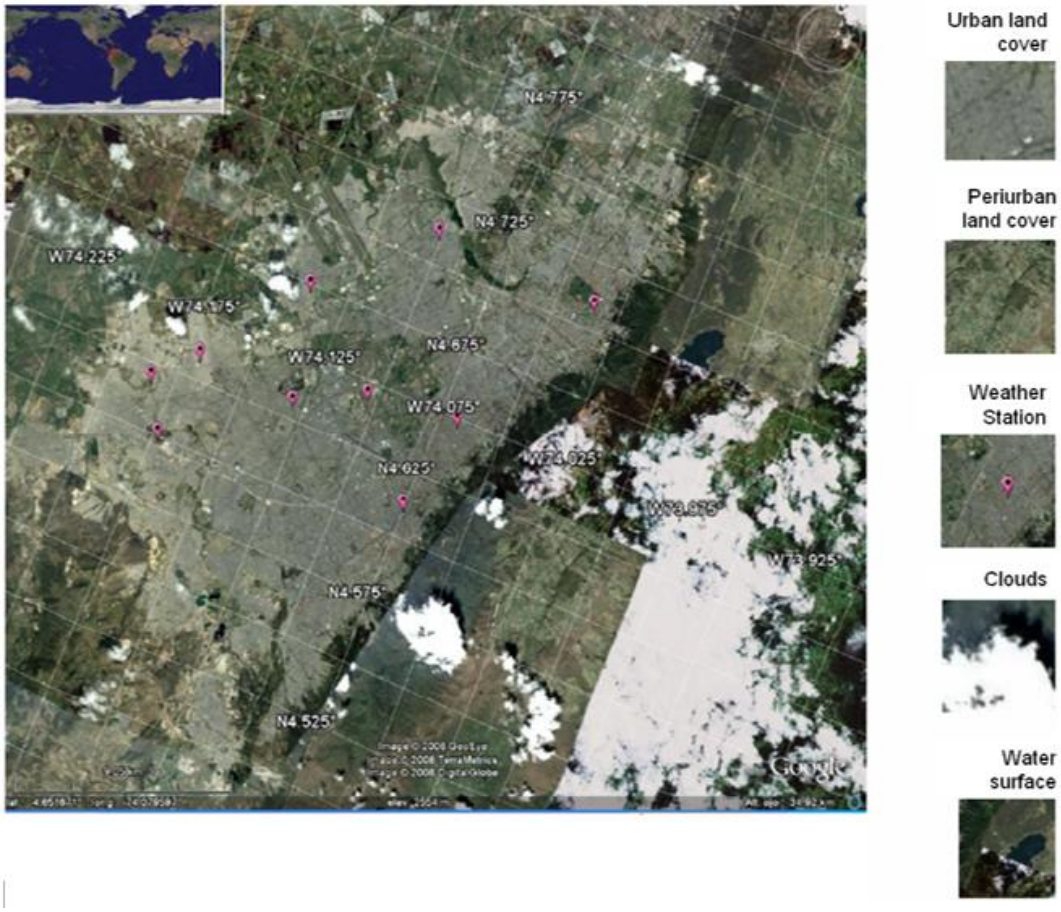

Figure1. *WeatherStationslocation (primary data: Google Earth)*

2.2 Satellite Data

The selected imagery were considered as auxiliary data for finding the heat islands and defining the spatial pattern changes of the thermal and infrared wave reflection in this city. All the imagery was obtained from the ETM+ sensor space born by Land sat 7 under clear sky conditions (cloud cover under 5%) or better, and downloaded from the Earth Explorer interface from NASA.

Due to the ETM+ sensor is technically damaged by the gaps presence [19], two images from 2007 were selected for modeling the thermal and infrared wave reflection in the specific dates: February 1st of 2007 (Fig. 2) and February 23 of 2007 (Fig. 3).

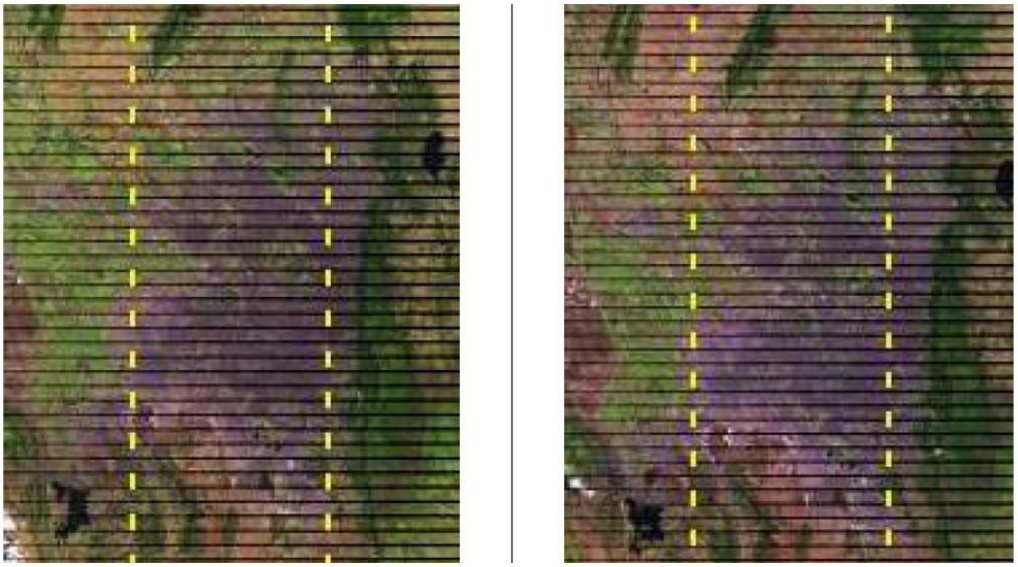

Figure2. *Bogota 8-57 LE70080572007038EDC00*

Figure3. *Bogota 8-57 LE70080572007054ASN00*

3. METHODS

This research was divided in two main phases for integrating the remote sensing images with the ground stations data. The first phase involved the statistical analysis of the air quality and weather data for building the empirical, semi-empirical and theoretical models using univariate time series selection.

The empiric model was designed for finding coefficients with significant correlation to the pollutants data for the whole year. Later, the semi-empirical model described the dynamic of the nitrous oxide and the nitrogenous dioxide in presence of solar light, which produces O_3, including the NOx natural cycle [20].Taking into account that the NO_2 photolysis is originated by the wave length radiation lesser than 424 nanometers the theoretical model helps to explain the O_3 genesis and its daily dynamic under atmospheric stability, humidity and the pollutants in the air [21].

In the time period from 5:00 h to 9:00 h, the hydrocarbons emission increases due to the combustion of fuel used for transportation and industrial activities for this city. When the solar radiation interacts with hydrogenous monoxide -NO, methane $–CH_4$ and non-methane hydrocarbons -NMHC, these pollutants are transformed into NO_2 and O_3, in particular, from 11:00 h to 15:00 h.

In order to model the O_3 cycle, such parameters as contaminant agents, humidity and atmospheric pressure were transformed using a numerical expansion in a histogram frequency (Equation 1)

$$\hat{y} = (z - z_{min}) / (z_{max}-z_{min}) * k \quad \text{(Equation 1)}$$

where, $\hat{y}$ is the transformed value, z is the initial value, $z_{min}$is the lowest range value from z values, z_{max} is the highest value from z values and, k is the inferential constant obtained from the mode of the highest hourly values of solar radiation.

The second phase involved the data satellite processing in combination with the results from the first phase statistical modeling through the exploratory data analysis. The procedure was developed for finding the spatial relationship between the pollutants presence and the wavelength reflection captured by ETM+ based in four 'theoretical assumptions':

The ultraviolet segment from the solar radiation is mostly absorbed by the ozone layer [22], which means that an ultraviolet piece is still transferred to the lowest atmosphere and it should be captured by the smog city layer.

The infrared radiation is absorbed and reemitted by the urban surface. It heats enough for producing changes in the wavelength radiation retained by the tropospheric ozone precursors [23] [24]. Then it should be possible to locate areas with more temperature and more infrared radiation emission. This could increase the probability of occurrence of the heat island effect.

When these theoretical assumptions are confirmed (1 and 2),it is possible to find spatial coincidences between the areas with high O_3 concentration and those with more temperature, indicating the radiative forcing effect of the pollutants.

Finally, the reduction of the solar radiation impacting the surface caused by the tropospheric ozone layer matches the areas with more temperature and infrared emission in the urban context, which indicates a possible dimming phenomenon.

In order to find the major amount of information coming from the ultraviolet, infrared and thermal infrared wavelengths derived from ETM+ sensor, the spatial exploration used the geometric transformation knows as "Principal Component Analysis". This decomposition was simultaneously applied to every band of the original image resulting into a different multispectral image. This procedure is also known as Karhunen-Loève [25] and the outsource image is referred to a generated space by vectors in direction to principal components from the original image.

The selected electromagnetic wave range was derived from the ETM+ imagery in the values for infrared (0.78 – 0.9; 1.55 – 1.75 and 2.09 – 2.39 μm) and thermal infrared (10.4 – 12-5 μm). It should be noticed that the UV range was not successfully studied due to the default wave range captured by this sensor.

4. RESULTS AND DISCUSSION

4.1 Solar Radiation and Its Correlation Coefficients

The contamination agents interfering the solar radiation –SR, were studied using the Pearson's method (r) for building the empiric, semi-empiric and theoretical models. The highest correlation with SR were found between global SR-O_3 (r = 0.79) and Ultraviolet B-O_3 (r = 0.74). This explains

the O3 genesis when the SR factor also includes the correlation between temperature and O_3 (r = 0.9). The correlation coefficient of the global SR and UV-B with other pollutants were: SO_2 (-0.32, -0.4), CO (-0.45, -0.5), NO (-0.16, -0.24), NO_2 (-0.2, -0.23), PM10 (-0.21, -0.28), NOx (-0.21, -0.27), which means they are not significantly correlated to SR at least in the whole day period.

4.2 Approaching for a Daily Local Dimming Model

In this case, the local dimming model related to the heat island effect in this urban area was not an inductive process but a deductive process, mainly because this phenomenon is not representative for all dates during such large time period. The availability of clear sky ETM+ imagery for analyzing solar radiation data was one of the most problems of this research.

Nevertheless, a behavior was observed in the spatial distribution of O_3, global SR and temperature using the information from the ground weather stations. Figure4 and Figure5 are maps showing the absence of the dimming phenomenon for the city in early afternoon hours (13:00 h). This situation changes when the dimming phenomenon is observed due to increasing presence of the O_3, which captures an important portion of the solar radiation during the mid-afternoon hours (15:00 h) as shown in Figure6 Figure7.

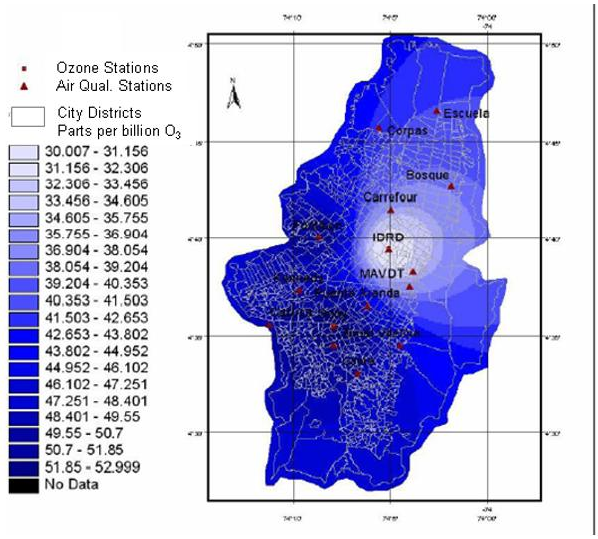

Figure4. *Troposphere O_3distribution*

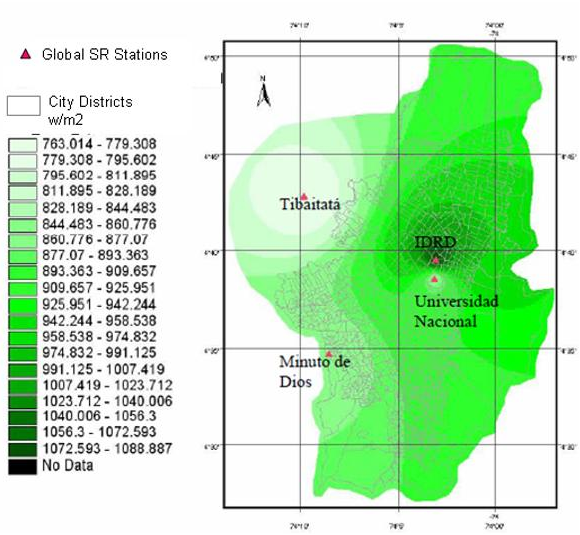

Figure5. *Global Solar Radiation on surface*

As shown in Fig. 4 and 5, the IDRD weather station records the highest global SR and the lowest O_3 presence. Due to O_3 cycle's top is not achieved until 12:00 h, there are not relevant data for detecting the dimming especially in the morning and even in the early-afternoon hours.

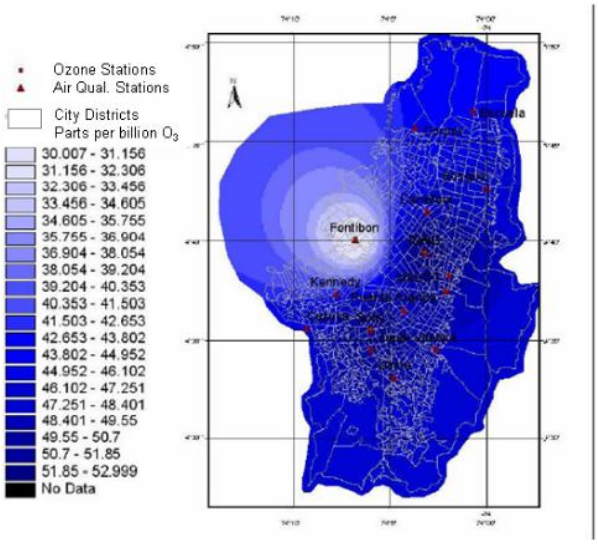

Figure6. *Tropospheric O_3distribution*

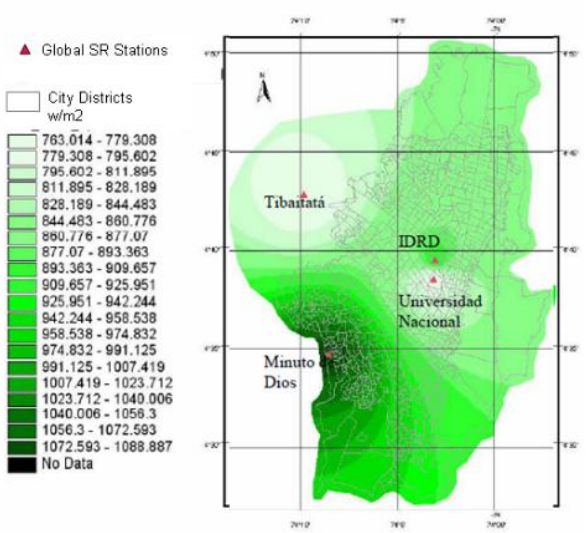

Figure7. *Global Solar Radiation on surface*

As depicted in Fig. 6 and 7, a common spatial pattern appears in O_3 and global SR distribution during mid-afternoon hours: the spatial areas where O_3 gets higher values are the same areas with lower global Solar Radiation values for the city.

4.3 Theoretical Assumptions

For analyzing traces of the ultraviolet portion (0.45 μm – 0.61 μm) through ETM+ sensor, the eigenvectors were processed, and as expected, none of the components showed if UV was affected by tropospheric ozone, so the first theoretical source was not supported by using remote sensing (Figure8 and Figure9) and only weather stations data were finally valid.

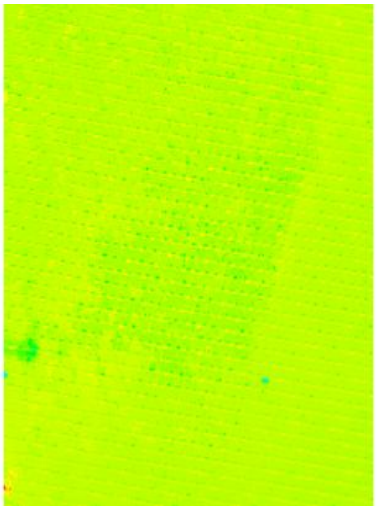

Figure8. *Secondeigenvector*

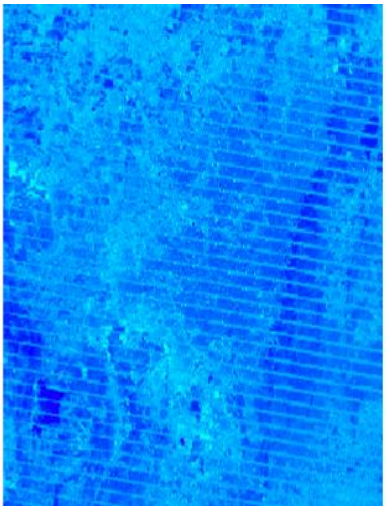

Figure9. *Thirdeigenvector*

For the infrared portion analysis (0.78 μm – 0.9 μm, 1.55 μm – 1.75 μm and 2.09 μm – 2.39 μm), the first component included 94% information depicting differential areas for the infrared emission. In the Fig. 10, the medium infrared emission areas are located in the east gap of the city corresponding to the mountain forest, while low emission zones are indicated by the numbers (1 and 2).

In combination with the higher O_3 values (Fig. 6) and the less infrared emission, it is possible to observe the effect of this pollutant as capturer of the infrared waves. This also corresponds to the descriptions about correlation between this pollutant and temperature [26][27].

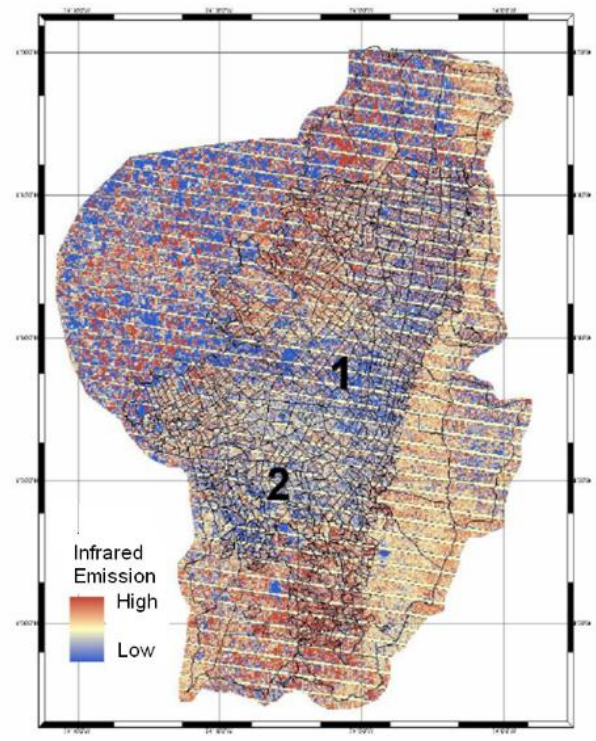

Figure10. *Infraredemission*

The Figure 11 shows the first component including 92% information of the thermal infrared wave derived from ETM+ sensor. In these images, differential areas are depicted where there is a high infrared thermal emission in the city. Two heat islands were indicated in the principal industrial district (Puente Aranda, number 2 inFigure 11) and the most traffic district area (Chapinero, number 2 inFigure 11) of the city of Bogota.

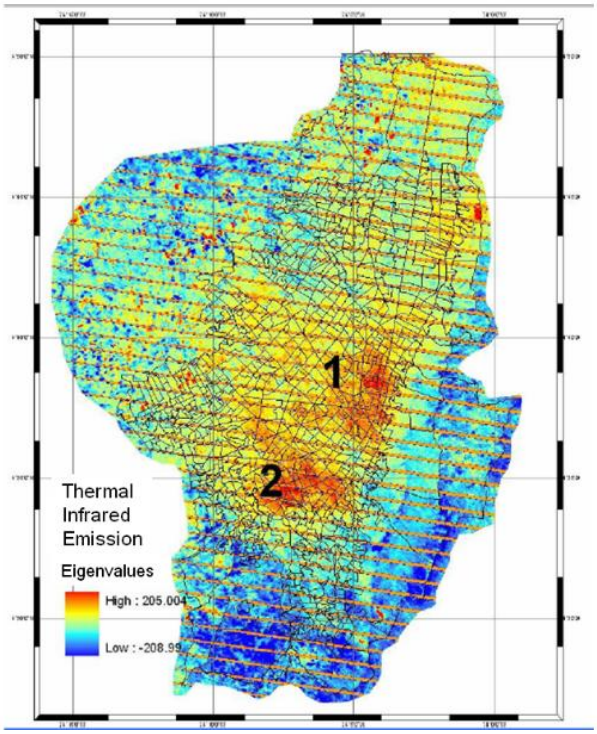

Figure 11.*Heatislandsdeducedbyusingeigenvaluesfromthermalinfrared data in thecity of Bogotá*

5. CONCLUSIONS

Eleven weather data stations in the city of Bogota were used to correlate several variables such as global radiation, atmospheric pressure, wind speed direction with the contamination agents as CO, SO, SO_2, particulates, NOx and O_3 during the 2007 year. During the exploratory air-quality analysis, high correlations were found among global Solar Radiation and O_3 (0.79), and UvB and O_3 (0.74), which describes the tropospheric ozone genesis under certain conditions of light and temperature.

The O_3 cycle modeling led to an urban dimming per-day model, which starts at the mid-day hours by the transformation of the pollutants under the solar radiation increase. In order to understand its spatial dynamic and possible effects on the temperature, the principal components of two ETM+ images were used for depicting the spatial distribution of the pollutant compared to the reduction of the solar radiation and UV-B after midday hours.

Concerning to the heat islands effect, two differential areas were recognized in the city of Bogota, located in the Chapinero and Puente Aranda districts. The first one holds the most transportation traffic and the second one is the industrial core of the Bogota's metropolitan area. This indication was based in the retention of infrared waves by the O_3 at mid-afternoon hours and contrasted to the IR low emission

This approach allows comparing the dimming and heat islands phenomena in the city and how they are spatially correlated with the smog layer. Because in Bogota, both phenomena appeared where the urban infrastructure and industrial areas are located, it is assumed that the tropospheric O_3 is rapidly produced by the traffic and the industrial activities, which begin in the morning growing faster with the passing of the hours and decreases after sunset.

As a way to sort the limitations of the satellite data techniques, as the mentioned clear sky condition, it was necessary to use auxiliary information like ground weather stations. This methodology uses deductive methods with acceptable results for modeling the spatial spread of the pollutants, especially in countries with dearth access to well-distributed climatological ground data.

This research becomes an approach for understanding the relationship between two processes of the Earth system: global dimming and heat islands in an urban context. Due to the effects of the global dimming phenomenon cannot be absolutely explained as consequence of the human action without taking into account the heat islands phenomenon, there is a compelling need to address the study of the Climate Change combining air quality modeling and satellite imagery for a deep understanding.

ACKNOWLEDGEMENTS

Thanks to RMCAB and the IDEAM for the meteorological and contaminants data. To Elena Posada from the the InstitutoGeográfico Agustin Codazzi,for spatial modeling using remote sensing and Ing. Luisa Pinzón for GIS resources.

REFERENCES

[1] Noyes, P. D., M. K. McElwee, H. D. Miller, B. W. Clark, L. A. Van Tiem, K. C. Walcott, K. N. Erwin and E. D. Levin (2009). "The toxicology of climate change: Environmental contaminants in a warming world." Environment international 35(6): 971-986.

[2] Meleux, F., F. Solmon and F. Giorgi (2007). "Increase in summer European ozone amounts due to climate change." Atmospheric Environment 41(35): 7577-7587.

[3] Lohmann, L. (2009). When markets are poison: learning about climate policy from the financial crisis, Corner House.

[4] Chung, E.-S., B. Soden, B. J. Sohn and L. Shi (2014). "Upper-tropospheric moistening in response to anthropogenic warming." Proceedings of the National Academy of Sciences 111(32): 11636-11641.

[5] Schmidt, G. A., D. T. Shindell and K. Tsigaridis (2014). "Reconciling warming trends." Nature Geosci 7(3): 158-160.

[6] Andreae, M. O., C. D. Jones and P. M. Cox (2005). "Strong present-day aerosol cooling implies a hot future." Nature 435(7046): 1187-1190.

[7] Jaeglé, L., D. J. Jacob, W. H. Brune and P. O. Wennberg (2001). "Chemistry of HOx radicals in the upper troposphere." Atmospheric Environment 35(3): 469-489.

[8] Jaramillo Ayerbe, M., D. E. González Gómez, M. E. Núñez Cabrera, G. E. Portilla and J. H. Lucio García (2007). "Univariant time series analysis applied to ozone forecasting in the city of Cali, Colombia." Facultad de Ingeniería Universidad de Antioquia Journal: 79-88.

[9] Burnett, R. T., J. R. Brook, W. T. Yung, R. E. Dales and D. Krewski (1997). "Association between ozone and hospitalization for respiratory diseases in 16 Canadian cities." Environmental research 72(1): 24-31.

[10] Uysal, N. and R. M. Schapira (2003). "Effects of ozone on lung function and lung diseases." Current opinion in pulmonary medicine 9(2): 144-150.

[11] Takagi, M. and K. Gyokusen (2004). "Light and atmospheric pollution affect photosynthesis of street trees in urban environments." Urban forestry & urban greening 2(3): 167-171.

[12] Stanhill, G. and S. Cohen (2001). "Global dimming: a review of the evidence for a widespread and significant reduction in global radiation with discussion of its probable causes and possible agricultural consequences." Agricultural and Forest Meteorology 107(4): 255-278.

[13] Alpert, P., P. Kishcha, Y. J. Kaufman and R. Schwarzbard (2005). "Global dimming or local dimming?: Effect of urbanization on sunlight availability." Geophysical Research Letters 32(17).

[14] Stanhill, G. and S. Cohen (2009). "Is solar dimming global or urban? Evidence from measurements in Israel between 1954 and 2007." Journal of Geophysical Research: Atmospheres 114(D10): D00D17.

[15] Alpert, P. and P. Kishcha (2008). "Quantification of the effect of urbanization on solar dimming." Geophysical Research Letters 35(8): L08801.

[16] Wang, K., H. Ye, F. Chen, Y. Xiong and C. Wang (2012). "Urbanization effect on the diurnal temperature range: different roles under solar dimming and brightening*." Journal of Climate 25(3): 1022-1027.

[17] Tanaka, K., A. Imamovic, D. Folini, A. Ohmura and M. Wild (2013). Is global dimming and brightening limited to urban areas? EGU General Assembly Conference Abstracts.

[18] Peters, W., M. Krol, F. Dentener, A. Thompson and J. Lelieveld (2001). "Chemistry-transport modeling of the satellite observed distribution of tropical tropospheric ozone." Atmospheric Chemistry and Physics Discussions 1(2): 337-378.

[19] Wulder, M. A., J. C. White, S. N. Goward, J. G. Masek, J. R. Irons, M. Herold, W. B. Cohen, T. R. Loveland and C. E. Woodcock (2008). "Landsat continuity: Issues and opportunities for land cover monitoring." Remote Sensing of Environment 112(3): 955-969.

[20] Seinfeld, J. H. and S. N. Pandis (2012). Atmospheric chemistry and physics: from air pollution to climate change, John Wiley & Sons.

[21] Saito, S., I. Nagao and H. Tanaka (2002). "Relationship of NOx and NMHC to photochemical O3 production in a coastal and metropolitan areas of Japan." Atmospheric Environment 36(8): 1277-1286.

[22] Vuilleumier, L., R. A. Harley, N. J. Brown, J. R. Slusser, D. Kolinski and D. S. Bigelow (2001). "Variability in ultraviolet total optical depth during the Southern California Ozone Study (SCOS97)." Atmospheric Environment 35(6): 1111-1122.

[23] Sherwood Rowland, F. (1990). "Earth's changing atmosphere: chlorofluorocarbons and ozone." Environmental Impact Assessment Review 10(4): 359-370.

[24] Baker, A. K., A. J. Beyersdorf, L. A. Doezema, A. Katzenstein, S. Meinardi, I. J. Simpson, D. R. Blake and F. Sherwood Rowland (2008). "Measurements of nonmethane hydrocarbons in 28 United States cities." Atmospheric Environment 42(1): 170-182.

[25] Hashimoto, N., Y. Murakami, P. A. Bautista, M. Yamaguchi, T. Obi, N. Ohyama, K. Uto and Y. Kosugi (2011). "Multispectral image enhancement for effective visualization." Optics Express 19(10): 9315-9329.

[26] Meleux, F., F. Solmon and F. Giorgi (2007). "Increase in summer European ozone amounts due to climate change." Atmospheric Environment 41(35): 7577-7587.

[27] Noyes, P. D., M. K. McElwee, H. D. Miller, B. W. Clark, L. A. Van Tiem, K. C. Walcott, K. N. Erwin and E. D. Levin (2009). "The toxicology of climate change: Environmental contaminants in a warming world." Environment international 35(6): 971-986.

AUTHOR'S BIOGRAPHY

Dr. Ricardo, CASTRO-DIAZ, Geographer (UNAL-Colombia), Specialized in Climate Change and Kyoto Protocol (ILC-Peru/Spain), Specialized in Application Development using Remote Sensing and GIS (CDAC-India), MSc. in Geomatics (UNAL-Colombia) and Doctor in Geography (UBA-Argentina). He is a researcher of the Institute of Geography "Dr. Romualdo Ardissone" of the School of Philosophy and Letters of the University of Buenos Aires (Argentina). His research lines are Climate Change and Remote Sensing, Complex Social-ecological system analysis and Environmental Services Studies. At present, he is granted by the National Council of Scientific and Technological Researches of Argentina (CONICET).